J Appl Electrochem (2009) 39:995–1001
DOI 10.1007/s10800-008-9747-4

ORIGINAL PAPER

Performance of lithium-ion cells with a γ-ray radiated electrolyte

N. Ding · X. Fang · J. Xu · Y. X. Yao · J. Zhu · C. H. Chen

Received: 9 May 2008 / Accepted: 2 December 2008 / Published online: 30 December 2008

Abstract Lithium-ion cells are potential energy storage devices in planetary exploration due to their high energy density and long lifespan. The high intensity of γ-ray radiation in outer space poses a great challenge to lithium-ion cells. In this study, radioactive Co-60 was applied as the radiation source to investigate the performance of lithium-ion cells with the electrolyte radiated by γ-rays. Two kinds of cathode ($LiMn_2O_4$, $LiNi_{0.8}Co_{0.15}Al_{0.05}O_2$) and three kinds of anode (Li, graphite, $Li_4Ti_5O_{12}$) were examined. There are two new mechanisms in the cells with a radiated electrolyte which affect the cell voltage and cycling performance: (i) erosion of the lithium electrode in the radiated electrolyte in the cases of half cells and lithium symmetrical cells; and (ii) electrochemical reaction between carboxyl species and the lithium extracted from the cathode in the case of full cells.

Keywords Radiation · Lithium-ion battery · Aerospace · Electrolyte · Electrochemical performance

1 Introduction

Rechargeable lithium-ion cells with high energy density are currently being investigated as an important power source for spacecraft [1]. However, the extreme environment in outer space with extremely low temperature and high vacuum affects the performance of lithium-ion cells. There have been several studies of battery performance at low temperatures [2, 3]. In addition to the low temperature and high vacuum, there is also the question of radiation in outer space. On average, high-power radiation bursts occur three times each day. Some celestial bodies, such as Jupiter, with a strong magnetic field, can also generate a deadly radiation environment [4]. Over the past five years, the Electrochemical Technologies Group of the U.S. Jet Propulsion Laboratory and the Institute of Space Technology and Aeronautics of Japan Aerospace Exploration Agency have published a series of papers in this field [5–10].

As a lithium-ion cell is composed of cathode, anode, separator and electrolyte, it is necessary to evaluate separately their individual responses to the radiation environment. In previous papers, we have reported the influence of radiation on cathode material ($LiCoO_2$) and the whole cells [11, 12]. In this study, we focused on the influence of radiation on the electrolyte and its consequence for cell performance.

2 Experimental

The electrolyte was a solution of 1 M $LiPF_6$ dissolved in EC/DEC (1:1, w/w) where EC and DEC stand for ethylene carbonate and diethyl carbonate, respectively. Before the electrolyte was used in making electrochemical cells, it was brought to a radiation chamber of a Co-60 facility with a radiation intensity of 5×10^4 Ci. The radiation lasted for 20 h at a high dosage rate of 100 Gy min^{-1}. Electron paramagnetic resonance (ESR) spectroscopy was employed with a JEOL JES-FA200 spectrometer.

Laminates of lithium metal oxides ($LiMn_2O_4$, $LiNi_{0.8}Co_{0.15}Al_{0.05}O_2$) and graphite were used as the positive and negative electrodes, respectively. The positive electrode consisted of a mixture of 84 wt% of active material

N. Ding · X. Fang · J. Xu · Y. X. Yao · J. Zhu · C. H. Chen (✉)
Department of Materials Science and Engineering, University of Science and Technology of China, Hefei, Anhui 230026, People's Republic of China
e-mail: cchchen@ustc.edu.cn

($LiMn_2O_4$ from Ningbo Huatian Co. and $LiNi_{0.8}Co_{0.15}Al_{0.05}O_2$ from Argonne National Lab), 8 wt% of carbon black and 8 wt% of PVDF binder. The negative electrode consisted of 90 wt% of graphite (Yuyao, Zhejiang) and 10 wt% of PVDF. $Li_4Ti_5O_{12}$ was also used as a negative electrode for a comparative study. $Li_4Ti_5O_{12}$ was synthesized via a solid state reaction process using Li_2CO_3 and TiO_2 as starting materials. The mixture was first calcined at 800 °C for 12 h and then further sintered at 900 °C for 24 h. Similarly, the negative electrode of $Li_4Ti_5O_{12}$ consisted of 84 wt% of $Li_4Ti_5O_{12}$, 8 wt% of carbon black and 8 wt% of PVDF binder.

Coin cells (CR 2032 type) with the symmetrical-cell configurations (Li/Li and $LiMn_2O_4/LiMn_2O_4$), or with the full cell configuration (cathode/graphite), or with the half cell configuration (cathode/Li) were assembled in an argon-filled dry-box (MBraun Labmaster 130) with a porous polypropylene membrane (Celgard 2400) as the separator. Both pristine and the above-mentioned radiated electrolytes were used in these cells for comparison.

Electrochemical tests were carried out on a multi-channel battery test system (NEWARE BTS-610) in the galvanostatic charge–discharge mode. The AC impedance spectra were measured using a CHI 604A electrochemical workstation. The applied AC signal was 5 mV in the frequency range 1 mHz–100 kHz. All the AC impedance spectra were measured at the fully charged state of the cells.

3 Results and discussion

3.1 Effects of γ-radiation on electrolyte

After radiation, the color of the electrolyte turned brown from its originally colorless state. ESR spectra (Fig. 1) show that there are no stabilized radicals and all signals come from water. We have observed that if the pure EC-DEC solvent (without $LiPF_6$) or an electrolyte using other lithium conducting salts, such as lithium bis(oxalato)borate (LiBOB), is exposed to γ-radiation, the color does not change. Thus, the conducting salt, $LiPF_6$, must play a role in the discoloration of the radiated electrolyte. In fact, this phenomenon (color change) is similar to the effect of a thermal treatment on the electrolyte, where the color change is associated with the formation of oligoethylene oxides [$OPF_2(OCH_2CH_2)_nF$] [13, 14]. The Lewis acid property of PF_5 formed from the decomposition of $LiPF_6$ induces a ring-opening polymerization of EC and leads to the formation of PEO-like polymers as mentioned above.

The electrolyte resistance at ambient temperature was measured by AC impedance spectra of steel/steel symmetrical cells. The impedance of the cell with the radiated electrolyte (test cell) is about 0.2 ohm higher than that with the pristine electrolyte (standard cell), as shown in Fig. 2. The low conductance of radiated electrolyte may be related to the existence of PEO-like polymers, which increase the viscidity of electrolyte and block the Li-ion transport.

3.2 Li/Li symmetrical cells

Li/Li symmetrical cells were cycled at 0.2 mA cm^{-2} with each cycle lasting for 4 h (2 h for charge followed by 2 h for discharge). The voltage profiles of Li/Li symmetrical cells are shown in Fig. 3. The initial voltage of the standard cell is about 0.1 V, whereas it is about 1.08 V for the test cell. In addition, the voltage profile varies smoothly and periodically for the standard cell, but changes drastically for the test cell, especially in the first several cycles. This phenomenon can be attributed to the lithium erosion by the radiated electrolyte. In our previous

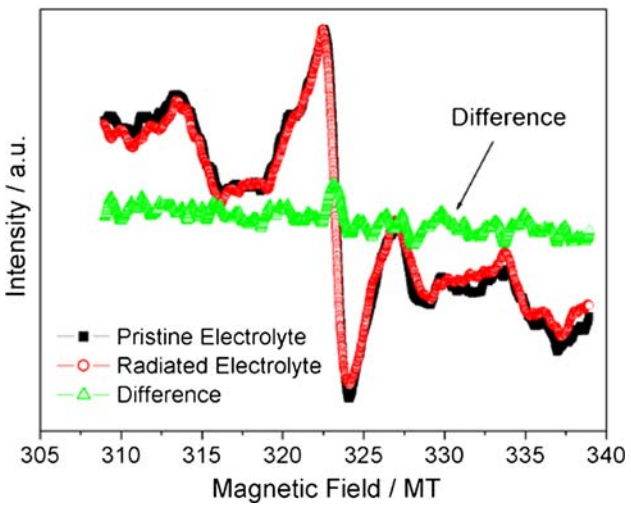

Fig. 1 ESR spectra of pristine and radiated electrolyte solutions

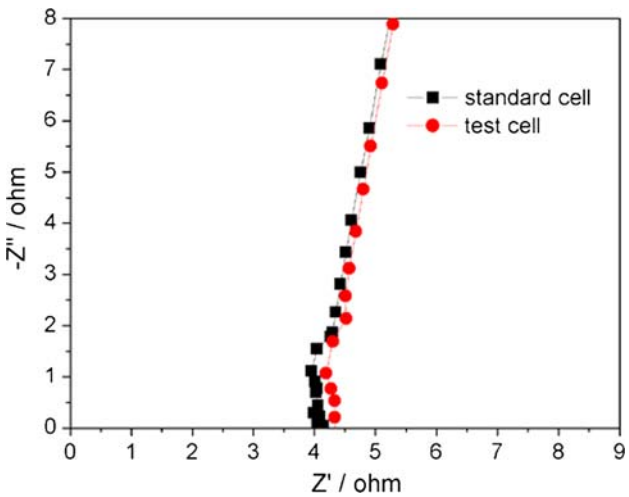

Fig. 2 Nyquist plots of steel/steel symmetrical cells

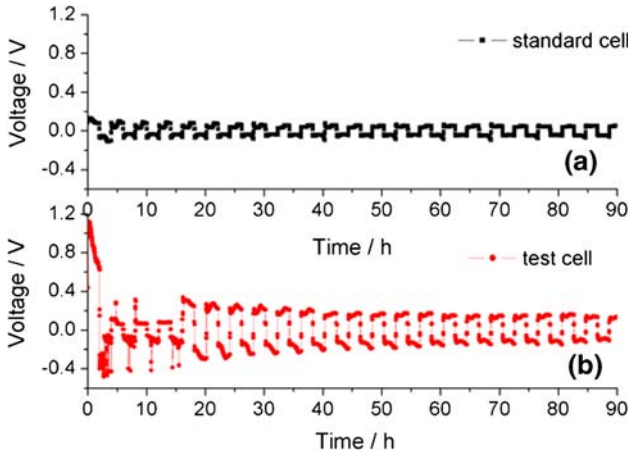

Fig. 3 Charge and discharge profiles of Li/Li symmetrical cells. The current density was 0.2 mA cm^{-2} with each cycle lasting 4 h

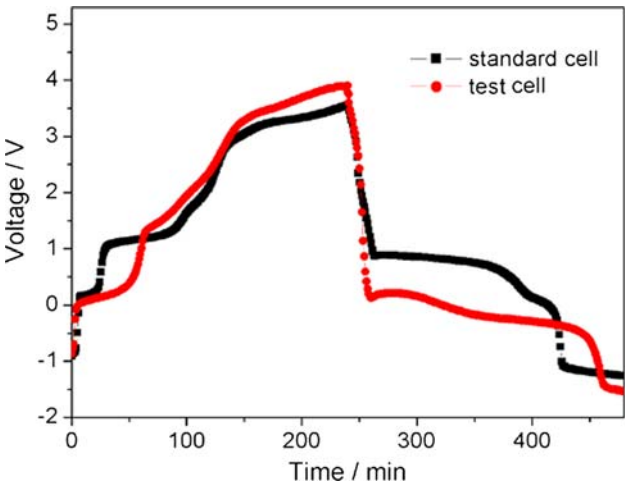

Fig. 4 Charge and discharge profiles of $LiMn_2O_4/LiMn_2O_4$ symmetrical cells. The current density was 0.2 mA cm^{-2} with each cycle lasting 8 h

paper, the carboxyl group (–COOH) has been detected in the radiated electrolyte by ^1H NMR spectroscopy [12]. The reaction between a carboxyl group and Li can cause large fluctuations on the voltage profile in the early cycles. In the subsequent cycles, the variation of the voltage profile of the test cell becomes stable. The stable voltage profile is probably due to precipitates formed on the lithium surface during the erosion, which can work as the solid state interface (SEI) film and prevent further erosion so that the cell becomes stabilized. However, due to the erosion, the voltage of the test cell is still about 0.12 V after 90 h, almost twice that of the standard cell (Fig. 3).

3.3 $LiMn_2O_4/LiMn_2O_4$ symmetrical cells

$LiMn_2O_4/LiMn_2O_4$ symmetrical cells were cycled at 0.2 mA cm^{-2} with each cycle lasting for 8 h (4 h for charge followed by 4 h for discharge). The first cycle voltage profiles of the cells with pristine and radiated electrolytes are shown in Fig. 4. They are similar in shape but different in voltage values; this can be attributed to the difference in the resistance of the two electrolytes, as shown in Fig. 2. Because of the lower conductance of the radiated electrolyte, the test cell exhibits a higher voltage during charge and a lower voltage during discharge. However, in the beginning period of charge (less than 50 mins), the voltage of the test cell is lower, which can be attributed to the effect of carboxyl species that exist in the radiated electrolyte. When lithium ions are extracted from the "cathode" $LiMn_2O_4$, they cannot all be inserted into the "anode" $LiMn_2O_4$, but, instead, react with the carboxyl species on the "anode". Therefore, the potential of the "anode" $LiMn_2O_4$ is higher, leading to a lower initial cell voltage.

3.4 $LiMn_2O_4$/Li and $LiNi_{0.8}Co_{0.15}Al_{0.05}O_2$/Li half cells

$LiMn_2O_4$/Li cells were cycled at a current density of 0.2 mA cm^{-2} in the voltage range from 3.3 to 4.5 V for the first three cycles and from 3.3 to 4.35 V for the subsequent cycles. As shown in Fig. 5, the charge voltage of the test cell is 0.35 V higher than that of the standard cell, which corresponds to the result of the Li/Li symmetrical cells, where the test cell also exhibited large polarization (Fig. 3). In the subsequent cycles, the discharge capacity of the test cell increases gradually and, after 80 cycles, it is even higher than that of the standard cell (Fig. 6). This phenomenon implies that lithium erosion by radiated electrolyte has reached an equilibrium and the erosion product can even improve the cycling performance by forming a better SEI film on the surface of the electrodes, especially on the anode:

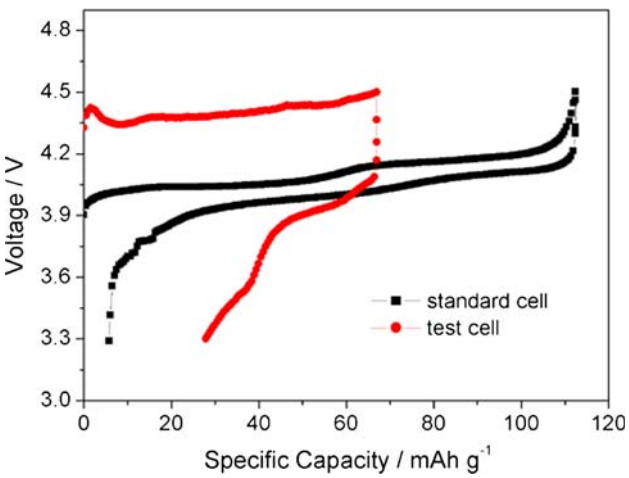

Fig. 5 Charge and discharge profiles of $LiMn_2O_4$/Li half cells in the voltage range between 3.3 and 4.5 V. The current density was 0.2 mA cm^{-2}

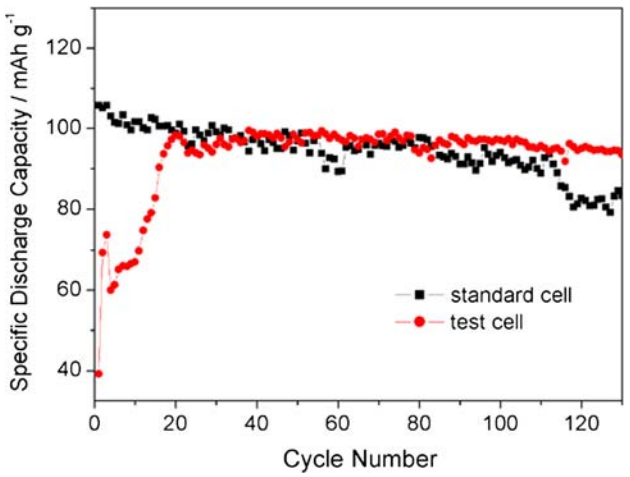

Fig. 6 Cycling performance of $LiMn_2O_4$/Li half cells. The voltage range was set between 3.3 and 4.5 V in the first three cycles and between 3.3 and 4.35 V in the subsequent cycles

more details will be discussed in the next full cell section [15]. In fact, some electrolyte additives such as SO_2 [16] and vinylene carbonate [17–20] have been used to enhance the formation of the SEI film. In addition, in the first cycle, the coulombic efficiency of the test cell is extremely low, just 58%, compared with 90% for the standard cell (Fig. 7). The much lower coulombic efficiency in the first cycle is due to the irreversible reaction between the radiated electrolyte and the Li anode. Although the capacity of the test cell can be recovered in the following cycle, its coulombic efficiency is still low, only 90%, compared with nearly 100% for the standard cell (Fig. 7). This constantly low efficiency can be attributed to a redox shuttle [13], as follows:

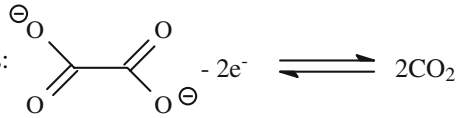

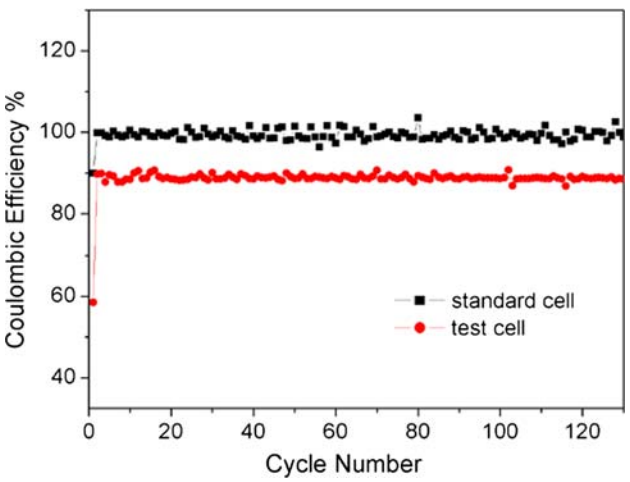

Fig. 7 Coulombic efficiency of $LiMn_2O_4$/Li half cells

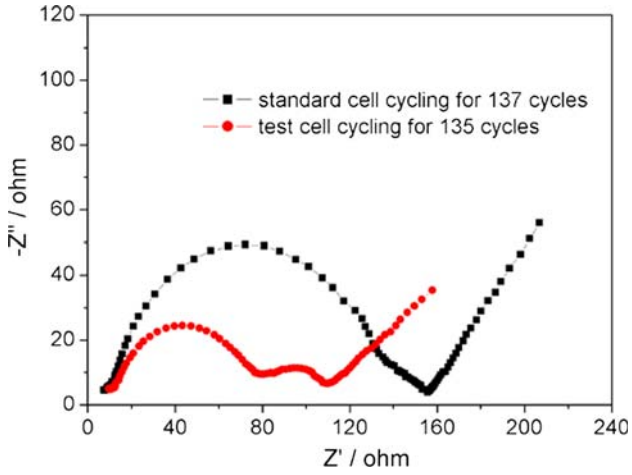

Fig. 8 Nyquist plots of $LiMn_2O_4$/Li half cells at the fully delithiated state (charged to 4.35 V)

The carboxyl group (oxalate, carbonate, or formate) can be oxidized to CO_2 on the cathode, instead of forming an SEI film on the anode (Li). And the product, CO_2 can be reduced to carboxyl group on the anode. This redox shuttle leads to a constantly low coulombic efficiency.

Nyquist plots of two fully charged $LiMn_2O_4$/Li cells (standard and test cell) are shown in Fig. 8. The total impedance of the standard cell is 154 ohm, which is much higher than that of the test cell (about 108 ohm). Furthermore, the impedance from the SEI film of the test cell (the first semi-circle in the high-frequency region in Fig. 8) is almost twice that of the standard cell. The significant impedance increase of the standard cell leads to lower capacity. More accurate results are calculated from the $LiNi_{0.8}Co_{0.15}Al_{0.05}O_2$/Li cells. The $LiNi_{0.8}Co_{0.15}Al_{0.05}O_2$/Li cells were cycled at a current density of 0.2 mA cm^{-2} between 2.8 and 4.2 V, with the cells being deliberately overcharged to 4.5 V in the first three cycles. Nyquist plots of $LiNi_{0.8}Co_{0.15}Al_{0.05}O_2$/Li cells are shown in Fig. 9 and the results fitted by an equivalent circuit (inset in Fig. 9) are summarized in Table 1. Along with the cell cycling, R_2 and R_3 of the test cell hardly change in contrast to those of the standard cell. The lower change of R_2 and R_3 is likely related to more stable SEI films on the electrodes induced by radiated electrolyte.

3.5 $LiMn_2O_4$/graphite and $LiNi_{0.8}Co_{0.15}Al_{0.05}O_2$/graphite full cells

In addition to half cells, full cells were also tested. To examine the effect of the cathodes, two cathode materials $LiMn_2O_4$ and $LiNi_{0.8}Co_{0.15}Al_{0.05}O_2$ were chosen. The first charge and discharge profiles of these two kinds of cell are shown in Fig. 10. A plateau at around 1.75 V is observed on the first charge curve of the test cells with both

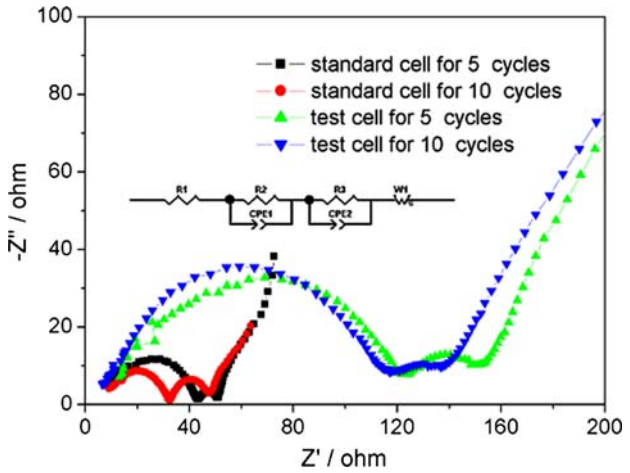

Fig. 9 Nyquist plot of $LiNi_{0.8}Co_{0.15}Al_{0.05}O_2$/Li half cells (the inset is the equivalent circuit used for the results fitting)

Table 1 Fitting results according to the equivalent circuit shown in Fig. 9

	Standard cell for 5 cycles	Standard cell for 10 cycles	Test cell for 5 cycles	Test cell for 10 cycles
R_1/Ω	5.85	7.07	11.43	7.71
R_2/Ω	38.29	25.97	113.9	105.3
CPE1-T	1.79E-05	2.28E-05	2.25E-05	1.50E-05
CPE1-P	0.677	0.71	0.665	0.763
R_3/Ω	5.5	12.24	21.78	21.06
CPE2-T	0.0089	0.009	0.005	0.0064
CPE2-P	1.04	0.978	0.948	0.725
W1-R	144.8	49.58	659.7	453.7
W1-T	851.3	225.7	1,012	469.7
W1-P	0.618	0.522	0.59	0.558

$LiMn_2O_4$ and $LiNi_{0.8}Co_{0.15}Al_{0.05}O_2$ as the cathodes. In the following cycles, the 1.75 V-plateau disappears, even if the cell is discharged to 1.6 V (Fig. 11). The origin of this 1.75 V-plateau is attributed to the radiated electrolyte.

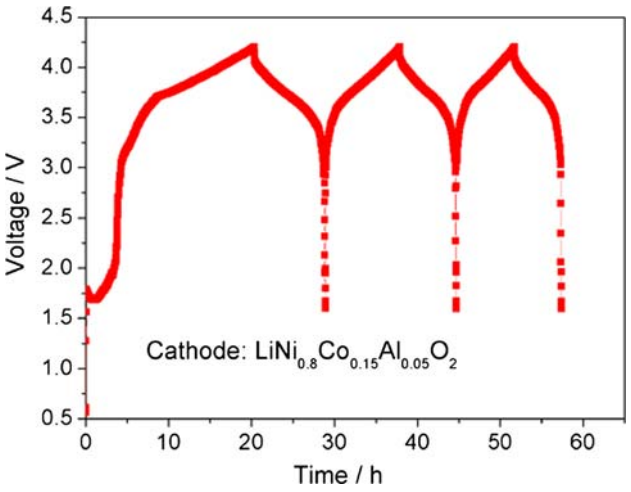

Fig. 11 Charge and deep discharge profiles of $LiNi_{0.8}Co_{0.15}Al_{0.05}O_2$/C full cells in the voltage range between 1.6 and 4.2 V. The current density was 0.2 mA cm^{-2}

Table 2 A proposed chemical reaction between the radiated electrolyte containing a carboxyl species and lithium for a thermodynamic calculation

Reaction	$HCOOH + Li \rightarrow HCOOLi + 1/2H_2$			
$\Delta_f H_m^\Theta / kJ\,mol^{-1}$	129	29.1	45.2	130.7
$S_m^\Theta / Jmol^{-1}K^{-1}$	–424.7	0	–608	0
Thermodynamic calculation	$\Delta G_m^\Theta = \Delta H_m^\Theta - T\Delta S_m^\Theta = -nE^\Theta F$			
	$E^\Theta = 1.75$ V			

Considering the existence of carboxyl species in the electrolyte, a thermodynamic calculation is used to estimate the voltage when a carboxyl species such as C_2H_5OCOOH reacts with lithium. The equation is written as shown in Table 2. Because no data of standard molar enthalpy and entropy of formation for C_2H_5OCOOH are available, HCOOH is used as a substitute. The equation is written as shown in Table 2. Also, in the thermodynamic calculation, the standard molar enthalpy and entropy of formation for

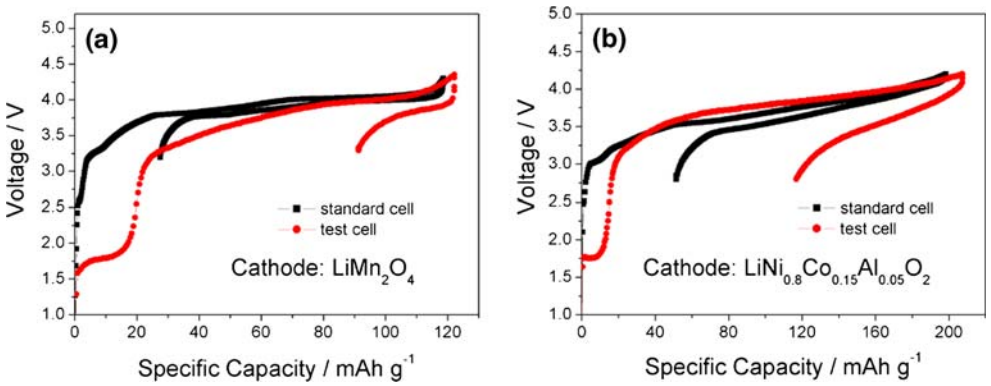

Fig. 10 Charge and discharge profiles of **a** $LiMn_2O_4$/C and **b** $LiNi_{0.8}Co_{0.15}Al_{0.05}O_2$/C full cells. The voltage range was between 3.3 and 4.35 V for $LiMn_2O_4$/C full cell and between 2.8 and 4.2 V for $LiNi_{0.8}Co_{0.15}Al_{0.05}O_2$/C full cell. The current density was 0.2 mA cm^{-2}

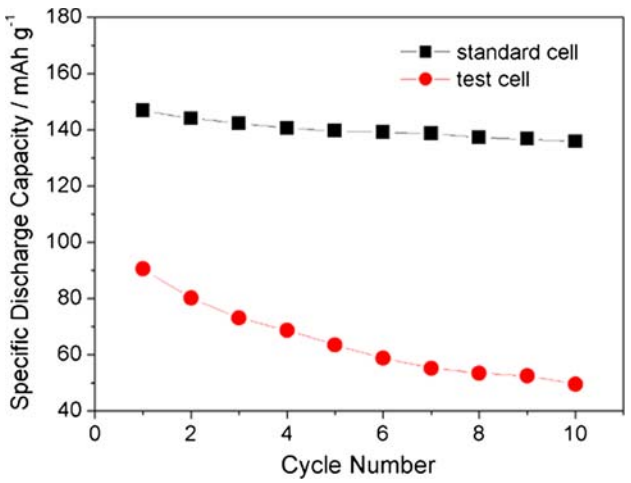

Fig. 12 Cycling performance of $LiNi_{0.8}Co_{0.15}Al_{0.05}O_2$/C full cells. The voltage range was between 2.8 and 4.2 V. The current density was 0.2 mA cm^{-2}

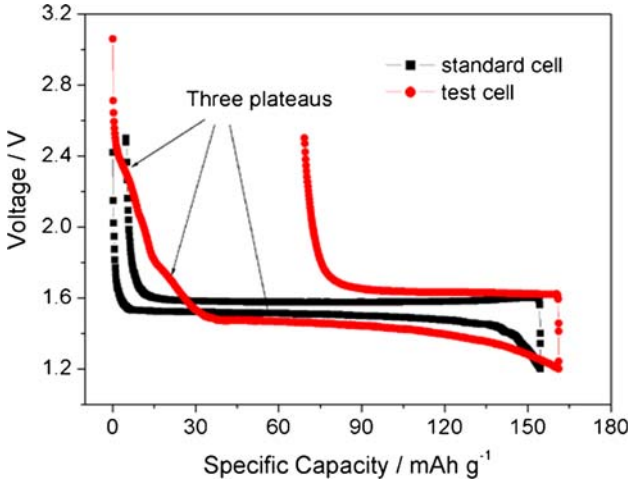

Fig. 13 Charge and discharge profiles of $Li_4Ti_5O_{12}$/Li cells. The voltage range was between 1.2 and 2.5 V. The current density was 0.067 mA cm^{-2}

HCOOLi are replaced by 50% of those for Li_2CO_3. The calculation result ($E^0 = 1.75$ V) is in good agreement with the experimental result. Because such a side reaction in the test cell consumes a certain amount of the active lithium source, the discharge capacity of the test cell is considerably lower than that of the standard cell. The cycling performance of the full cells is shown in Fig. 12. The capacity fading of the test cell is faster, and after 10 cycles, the capacity is only about one-third of that of the standard cell.

Obviously, the difference in the cycling performance of the half cells and the full cells with radiated electrolyte (Fig. 6 vs. Fig. 12) is mainly due to the choice of anode. For the half cells, the anode is highly active lithium metal, which can directly react with the carboxyl species in radiated electrolyte and form a dense SEI film on the lithium anode. This reaction is actually an erosion process. The formation of the SEI film increases the impedance of the half cell (Table 1) which leads to large polarization when the cell is cycled. Nevertheless, a dense SEI film also prevents further reaction between anode and electrolyte, and thus enhances the cyclability of half cells in the following cycles (Fig. 6). In addition, the lithium source is always excessive in a half cell so that the erosion reaction does not lead to a loss of cell capacity. However, for the full cells with radiated electrolyte, all active lithium comes from the cathode. The carboxyl existing in the electrolyte can consume a certain amount of active lithium and leads to capacity fading.

3.6 $Li_4Ti_5O_{12}$/Li cells

$Li_4Ti_5O_{12}$/Li cells were cycled at 0.067 mA cm^{-2} ($\sim$C/16 rate) in the voltage range 1.2–2.5 V. The first discharge and charge profiles are shown in Fig. 13. Three plateaus are observed in the first discharge curve of the test cell. The first plateau from 2 to 2.5 V may be attributed to the erosion of the lithium anode by the radiated electrolyte. The second plateau from 1.5 to 1.8 V is attributed to the reaction between the radiated electrolyte and the lithium intended for the $Li_4Ti_5O_{12}$, which corresponds to the explanation in the section on the full cells. The last plateau at about 1.5 V is the typical discharge plateau of $Li_4Ti_5O_{12}$ [21]. Because of the low conductance of the radiated electrolyte, the voltage of the test cell is slightly lower than that of the standard cell.

4 Conclusions

Aerospace exploration poses a challenge to the batteries as potential on-board power sources in terms of their tolerance to the high-radiation environment. Because lithium-ion cells are composed of cathode, anode, separator and electrolyte, it is important to evaluate individually their responses under the radiation environments. In this paper, we mainly focused on the performance of lithium-ion cells with the electrolyte after γ-ray radiation.

We found that the radiated electrolyte can erode the lithium anode and increase the impedance of Li/Li symmetrical cells. For $LiMn_2O_4$/Li half cells, although the initial capacity is low, the capacity of the cell using radiated electrolyte can be recovered and its cyclability can even be improved by forming a dense SEI film. A redox shuttle referring to carboxyl is proposed to explain the low columbic efficiency of $LiMn_2O_4$/Li test cells. For full cells of $LiMn_2O_4$/C and $LiNi_{0.8}Co_{0.15}Al_{0.05}O_2$/C, a voltage plateau at about 1.75 V, which is related to the reaction of carboxyl and lithium, appears in the first charge process

and disappears in the following cycles. Finally, lithium erosion and electrolyte reaction processes are further confirmed by $Li_4Ti_5O_{12}$/Li cells.

Acknowledgements This study was supported by the National Science Foundation of China (grant no. 50372064 and 20471057). The USTC radiation chemistry laboratory provided assistance for the experiments involving γ-ray radiation. We are also grateful to Dr. Andrew Jansen from Argonne National Laboratory for his help in language editing.

References

1. Ratnakumar BV, Smart MC, Kindler A, Frank H, Ewell R, Surampudi S (2003) J Power Sources 119:906
2. Plichta EJ, Behl WK (2000) J Power Sources 88:192
3. Wang LS, Huang YD, Jia DZ (2006) Solid State Ionics 177:1477
4. Fischer D (2001) Mission jupiter-the spectacular journey of the galileo spacecraft. Springer-Verlag, New York
5. Ratnakumar BV, Smart MC, Whitcanack LD, Davies ED, Chin KB, Deligiannis F, Surampudi S (2004) J Electrochem Soc 151:A652
6. Ratnakumar BV, Smart MC, Whitcanack LD, Davies ED, Chin KB, Deligiannis F, Surampudi S (2005) J Electrochem Soc 152:A357
7. Ratnakumar BV, Smart MC, Whitcanack LD, Ewell RC (2006) J Power Sources 159:1428
8. Ratnakumar BV, Smart MC, Whitcanack LD, Ewell RC, Whitcanack LD, Kindler A, Frank H, Narayanan SR, Surampudi S (2007) J Electrochem Soc 154:A715
9. Wang XM, Kato M, Naito H, Yamada C, Segami G, Kibe K (2006) J Electrochem Soc 153:A89
10. Wang XM, Sakiyama Y, Takahashi Y, Yamada C, Naito H, Segami G, Hironaka T, Hayashi E, Kibe K (2007) J Power Sources 167:162
11. Ding N, Zhu J, Yao YX, Chen CH (2006) Chem Phys Lett 426:324
12. Ding N, Zhu J, Yao YX, Chen CH (2006) Electrochim Acta 51:6320
13. Sloop SE, Kerr JB, Kinoshita K (2003) J Power Sources 119–121:330
14. Campion CL, Li W, Lucht BL (2005) J Electrochem Soc 152:A2327
15. Zhang SS, Xu K, Jow TR (2004) J Power Sources 130:281
16. EinEli Y, Thomas SR, Koch VR (1997) J Electrochem Soc 144:1159
17. Chen LB, Wang K, Xie XH, Xie JY (2007) J Power Sources 174:538
18. Lee HH, Wang YY, Wan CC, Yang MH, Wu HC, Shieh DT (2005) J Appl Electrochem 35:615
19. Ota H, Shima K, Ue M, Yamaki J (2004) Electrochim Acta 49:565
20. Moller KC, Santner HJ, Kern W, Yamguchi S, Besenhard JO, Winter M (2003) J Power Sources 119:561
21. Hao YJ, Lai QY, Xu ZH, Liu XQ, Ji XY (2005) Solid State Ionics 176:1201